Decoupled and semi-decoupled bands in ^{197}Hg and ^{199}Hg

D. Negi,[1] S. K. Tandel,[1,2,*] P. Chauhan,[1] P. Chowdhury,[2] R. V. F. Janssens,[3,4] M. P. Carpenter,[5] T. L. Khoo,[5] F. G. Kondev,[5] T. Lauritsen,[5] C. J. Lister,[2,5] D. Seweryniak,[5] and S. Zhu[5]

[1]*School of Physical Sciences, UM-DAE Centre for Excellence in Basic Sciences, University of Mumbai, Mumbai 400098, India*
[2]*Department of Physics, University of Massachusetts Lowell, Lowell, Massachusetts 01854, USA*
[3]*Department of Physics and Astronomy, University of North Carolina at Chapel Hill, Chapel Hill, North Carolina 27599, USA*
[4]*Triangle Universities Nuclear Laboratory, Duke University, Durham, North Carolina 27708, USA*
[5]*Argonne National Laboratory, Argonne, Illinois 60439, USA*

(Received 16 March 2019; revised manuscript received 11 April 2019; published 31 July 2019)

The structure of decoupled positive-parity and semidecoupled negative-parity bands up to high spin in ^{197,199}Hg has been studied using multinucleon transfer reactions with the Gammasphere array. A positive-parity band in ^{199}Hg with the $(\nu i_{13/2})^3$ decoupled configuration that deexcites to levels in the negative-parity sequences is newly established. The semidecoupled sequences in both isotopes are extended to higher spin. Rotation-aligned angular momenta and crossing frequencies determined from experiment are in fair agreement with those from cranking calculations. A transition from oblate collective rotation at low spin to triaxial noncollective shapes at high spin is indicated.

DOI: 10.1103/PhysRevC.100.014329

I. INTRODUCTION

Nuclei in the $A = 190$–200 region exhibit several interesting aspects of structure. In the Hf-Os ($Z = 72$–76) region, pronounced prolate deformation is evident near the ground state with a transition to oblate shapes at high spin around neutron number $N = 108$–110 [1,2]. Pt ($Z = 78$) isotopes exhibit triaxial shapes at low spin [3,4] whereas Hg ($Z = 80$) nuclei are characterized by oblate deformation [5–9] with Pb ($Z = 82$) isotopes being near spherical. The different mechanisms of coupling unpaired quasiparticles (qps) to the core are particularly evident in isotopes of Pt and Hg where decoupled and semidecoupled bands are observed. In oblate-deformed Hg isotopes along the line of stability, the neutron Fermi level lies in the vicinity of low-Ω orbitals from the $i_{13/2}$ subshell. Consequently, in odd-A Hg isotopes, a decoupled rotational band built on the $\nu i_{13/2}$ one-qp having a bandhead spin parity of $13/2^+$ is observed [5,10]. Semidecoupled bands, on the other hand, arise from the coupling of a low-j quasiparticle which is deformation aligned and high-j quasiparticles which are rotation aligned [11–13]. Such bands have been observed in previous studies of Pt and Hg isotopes [7,14–17]. Further high-spin data revealed the presence of rotation-aligned two-, three-, and four-qp band structures [10,16,18–32].

The high-spin structure of proton-rich Hg isotopes is well studied [10,19,23–27] including decoupled and semidecoupled bands. In contrast, information on isotopes around the line of stability is quite limited since these cannot be populated through fusion-evaporation reactions with a notable exception being the study of ^{200}Hg through an incomplete fusion reaction [28]. Specifically, the positive-parity yrast sequence built on the $13/2^+$ isomeric state in ^{199}Hg was known only up to the $I^\pi = 25/2^+$ level, which is below the region of the first band crossing, whereas the negative-parity band was established up to the $I^\pi = 31/2^-$ state [20]. In ^{197}Hg, the semidecoupled band was identified up to the $I^\pi = 33/2^-$ level [20]. It is of interest to establish the evolution of high-spin structure in heavier isotopes, particularly, the nature of band crossings and their role in angular momentum generation, approaching the $N = 126$ shell closure. Although fusion-evaporation reactions with stable beams are not feasible to populate high spin in these nuclei, multinucleon transfer reactions using heavy beams and targets at energies above the Coulomb barrier are suitable [33,34].

II. EXPERIMENTAL DETAILS AND DATA ANALYSIS

Excited states in ^{197}Hg and ^{199}Hg were populated through multinucleon transfer reactions with a 1450-MeV ^{209}Bi beam from the ATLAS accelerator at Argonne National Laboratory. A thick ($\approx$50 mg/cm^2) ^{197}Au target was used. The Gammasphere array [35] consisting of 100 Compton-suppressed high-purity germanium detectors was used to record three- and higher-fold coincidence events. The analysis of coincidence data was performed using the RADWARE suite of programs [36], and γ rays were placed in the level scheme on the basis of coincidence relationships and intensities. The directional angular correlation from oriented nuclei (DCO) technique [37] was used to assign spins of excited levels where sufficient data were available. DCO ratios were obtained using the

*Corresponding author: sktandel@gmail.com

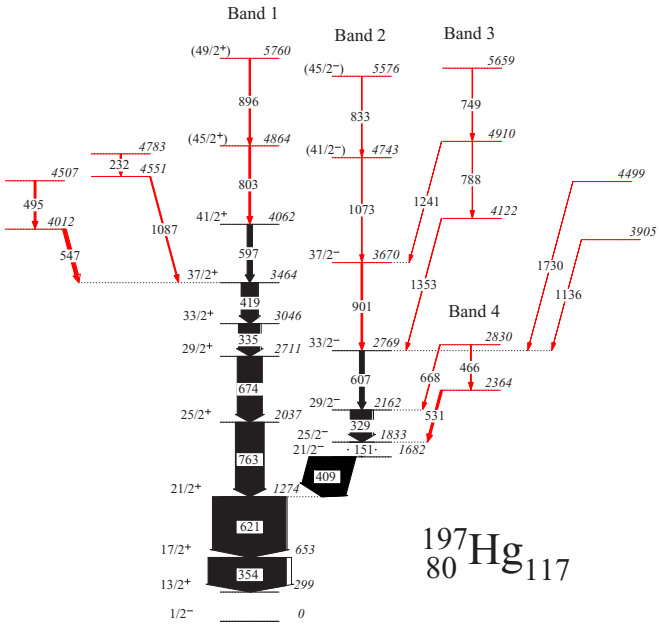

FIG. 1. Level scheme of ^{197}Hg obtained from the present work. The widths of the arrows are proportional to the relative intensities of the γ rays. The levels and transitions marked red are newly established.

relation,

$$R_{\mathrm{DCO}} = \frac{I(\gamma_1, \theta_1; \gamma_2, \theta_2)}{I(\gamma_1, \theta_2; \gamma_2, \theta_1)},$$

where $I(\gamma_1, \theta_1; \gamma_2, \theta_2)$ indicates the coincidence intensity of γ_1 and γ_2 detected at θ_1 and θ_2, respectively, and angles are defined with respect to the beam axis. In the present analysis, the choice of the angles was $\theta_1 = 30 \pm 10$ or 150 ± 10 and $\theta_2 = 90 \pm 10$, and γ_2 was chosen to have $E2$ multipolarity. If γ_1 has a pure stretched-quadrupole nature, then the DCO ratio is close to unity. On the other hand, if γ_1 has pure stretched-dipole nature, then the DCO ratio is close to 0.5. For a mixed transition, the ratio has an intermediate value dependent on the amount of dipole or quadrupole mixing. The applicability of the DCO technique in multinucleon transfer reactions with heavy-ion beams has already been demonstrated in our earlier work [31]. A search was also performed for possible metastable states with half-lives ranging from nanoseconds to microseconds; all excited levels, except the $13/2^+$ state, were determined to have half-lives of $T_{1/2} < 2$ ns.

III. RESULTS

Previous data on high-spin levels in ^{197,199}Hg were obtained using (α, xn) reactions on Pt targets [5,20]. The decay schemes reported from these experiments are now considerably extended with the inclusion of an additional 18 transitions and 16 levels in ^{197}Hg. In ^{199}Hg, 26 transitions and 18 levels are newly placed. The updated level schemes for ^{197}Hg and ^{199}Hg are displayed in Figs. 1 and 2. The observed γ rays in ^{197}Hg and ^{199}Hg along with their relative intensities, placements, and multipolarities where available are listed in

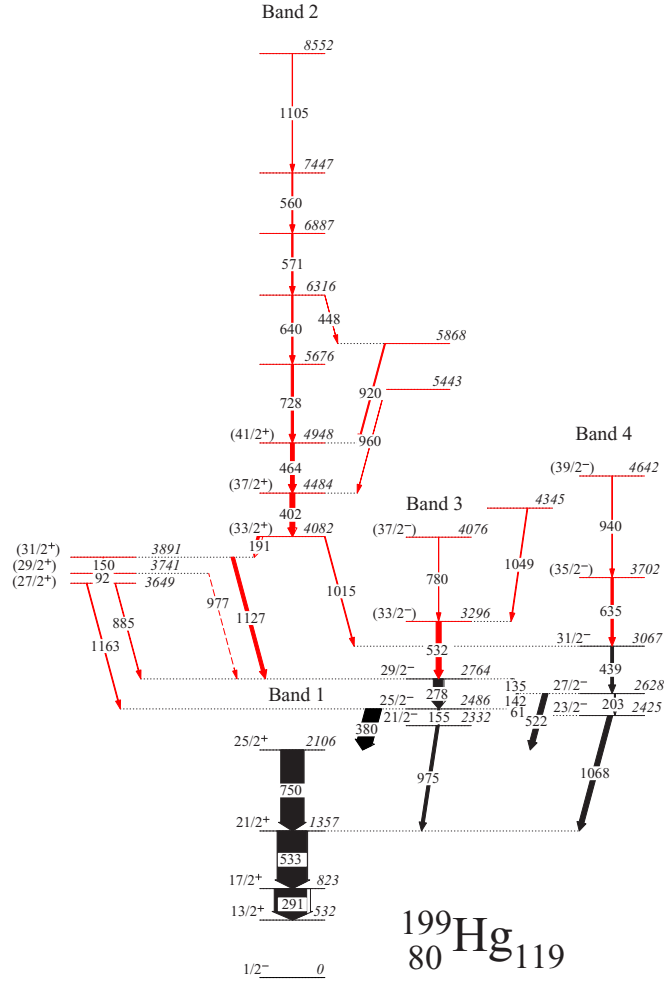

FIG. 2. Level scheme of ^{199}Hg obtained from the present work. The widths of the arrows are proportional to the relative intensities of the γ rays. The levels and transitions marked red are newly established.

Tables I and II, respectively. Detailed results for both nuclei are described below.

A. ^{197}Hg

1. Band 1

The positive-parity yrast band is extended up to the $(49/2^+)$ level with the inclusion of the 803-keV transition feeding the $41/2^+$ level at 4062 keV and the 896-keV γ ray being placed above the $45/2^+$ state. Representative spectra for transitions assigned to ^{197}Hg are displayed in Fig. 3. Both the 803- and 896-keV γ rays are assumed to have $E2$ multipolarity, similar to that of other lower-lying transitions in this band. Furthermore, the 547- and 1087-keV γ rays are observed to feed the $37/2^+$ level at 3464 keV. These two γ rays are, in turn, fed by the 495- and 232-keV transitions, respectively. Spin-parity assignments for these levels could not be determined. The unfavored signature partner of the decoupled band built on the $13/2^+$ state was not observed.

TABLE I. Energies and intensities of γ rays, energy of deexciting levels and spins of initial and final levels in ^{197}Hg. DCO ratios are obtained with a gate on the 354-keV $E2$ transition. γ-ray energies are accurate to within 0.5 keV. Statistical uncertainties on γ-ray intensities and DCO ratios are listed.

E_γ (keV)	I_γ	E_i (keV)	I_i^π	→	I_f^π	DCO
151.0	15.2(4)	1833.3	$25/2^-$	→	$21/2^-$	1.20(30)
231.6	1.5(1)	4782.6				
328.5	27.5(8)	2161.8	$29/2^-$	→	$25/2^-$	0.83(2)
334.8	27.0(8)	3045.5	$33/2^+$	→	$29/2^+$	0.79(2)
354.0	100.0(21)	653.0	$17/2^+$	→	$13/2^+$	
408.6	57.5(16)	1682.3	$21/2^-$	→	$21/2^+$	
418.8	21.3(6)	3464.3	$37/2^+$	→	$33/2^+$	1.04(3)
465.8	1.1(1)	2829.8				
495.4	2.4(1)	4506.9				
530.7	2.6(2)	2364.0		→	$25/2^-$	
547.2	3.9(2)	4011.7		→	$37/2^+$	
597.2	6.7(3)	4061.5	$41/2^+$	→	$37/2^+$	
607.0	6.1(3)	2768.8	$33/2^-$	→	$29/2^-$	1.01(4)
620.7	93.9(55)	1273.7	$21/2^+$	→	$17/2^+$	0.94(2)
668.0	0.8(2)	2829.8		→	$29/2^-$	
673.8	31.7(9)	2710.7	$29/2^+$	→	$25/2^+$	1.01(3)
763.2	36.4(11)	2036.9	$25/2^+$	→	$21/2^+$	0.80(2)
748.8	0.7(1)	5659.0				
788.2	0.5(1)	4910.2				
802.8	2.3(1)	4864.3	$(45/2^+)$	→	$41/2^+$	
833.3	0.4(1)	5576.2	$(45/2^-)$	→	$(41/2^-)$	
895.5	1.7(2)	5759.8	$(49/2^+)$	→	$(45/2^+)$	
900.9	2.1(2)	3669.7	$37/2^-$	→	$33/2^-$	1.03(15)
1073.2	0.5(1)	4742.9	$(41/2^-)$	→	$37/2^-$	
1086.6	1.5(1)	4551.0		→	$37/2^+$	
1135.8	0.4(1)	3904.6		→	$33/2^-$	
1240.7	0.2(1)	4910.2		→	$37/2^-$	
1353.2	0.6(1)	4122.0		→	$33/2^-$	
1730.2	0.3(1)	4499.0		→	$33/2^-$	

2. Band 2

Band 2 had been previously established up to the $33/2^-$ level [20]. Three new transitions with energies 901, 1073, and 833 keV are observed to be in coincidence with γ rays below the $33/2^-$ level and with each other (Fig. 3). Therefore, they are placed in cascade above the $33/2^-$ level in order of decreasing intensity. In addition, the 901-keV transition has been determined to be of quadrupole nature. The 1073- and 833-keV γ rays are assumed to have $E2$ multipolarity similar to the lower-lying transitions in this semidecoupled sequence. The relative placement of the two transitions may be considered ambiguous within intensity errors. Consequently, Band 2 is identified up to a probable $I^\pi = 45/2^-$ level.

3. Other transitions and levels

A new sequence of transitions with energies 1353, 788, and 750 keV is observed to be built on the $33/2^-$ state in Band 2. A 531-keV γ ray is seen to feed the $25/2^-$ level in Band 2 and is in coincidence with a 466-keV transition deexciting the 2830-keV level. Additionally, a 668-keV transition is observed to decay from this level to the $29/2^-$ one in Band 2.

TABLE II. Energies and intensities of γ rays, energy of deexciting levels, and spins of initial and final levels in ^{199}Hg. DCO ratios are obtained with a gate on the 291-keV $E2$ transition. γ-ray energies are accurate to within 0.5 keV. Statistical uncertainties on γ-ray intensities and DCO ratios are listed.

E_γ (keV)	I_γ	E_i (keV)	I_i^π	→	I_f^π	DCO
135.4	1.6(2)	2764.0	$29/2^-$	→	$27/2^-$	
142.1	1.8(2)	2628.3	$27/2^-$	→	$25/2^-$	
149.5		3890.6	$(31/2^+)$	→	$(29/2^+)$	
154.8	3.0(2)	2486.4	$25/2^-$	→	$21/2^-$	
191.0	7.3(5)	4081.6	$(33/2^+)$	→	$(31/2^+)$	0.51(10)
203.4	2.5(1)	2628.3	$27/2^-$	→	$23/2^-$	
277.6	28.9(13)	2764.0	$29/2^-$	→	$25/2^-$	0.94(3)
291.4	100.0(26)	823.4	$17/2^+$	→	$13/2^+$	
380.0	46.6(19)	2486.4	$25/2^-$	→	$25/2^+$	
402.0	14.4(7)	4483.6	$(37/2^+)$	→	$(33/2^+)$	0.85(3)
438.6	8.3(5)	3066.9	$31/2^-$	→	$27/2^-$	0.83(4)
447.9		6316.1				
464.3	11.3(6)	4947.9	$(41/2^+)$	→	$(37/2^+)$	0.94(4)
521.9	16.2(8)	2628.3	$27/2^-$	→	$25/2^+$	
532.0	15.2(8)	3296.0	$(33/2^-)$	→	$29/2^-$	
533.3	91.9(28)	1356.7	$21/2^+$	→	$17/2^+$	0.97(2)
560.0	2.9(2)	7446.9				
570.8	4.1(3)	6886.9				
635.1	7.1(4)	3702.0	$(35/2^-)$	→	$31/2^-$	
640.5	4.0(3)	6316.1				
727.7	6.7(5)	5675.6		→	$(41/2^+)$	
749.7	71.0(28)	2106.4	$25/2^+$	→	$21/2^+$	0.99(2)
779.8	0.8(1)	4075.7	$(37/2^-)$	→	$(33/2^-)$	
885.4	1.9(4)	3649.3	$(27/2^+)$	→	$29/2^-$	
920.0	3.4(3)	5867.9		→	$(41/2^+)$	
940.0	1.1(2)	4642.0	$(39/2^-)$	→	$(35/2^-)$	
959.8	0.7(2)	5443.4		→	$(37/2^+)$	
974.8	7.9(6)	2331.5	$21/2^-$	→	$21/2^+$	0.55(5)
(977.2)		3741.2	$(29/2^+)$	→	$29/2^-$	
1014.5	2.4(3)	4081.6	$(33/2^+)$	→	$31/2^-$	
1048.7	2.3(3)	4344.7		→	$(33/2^-)$	
1068.3	10.1(8)	2425.0	$23/2^-$	→	$21/2^+$	
1104.7	1.1(2)	8551.6				
1126.6	10.3(7)	3890.6	$(31/2^+)$	→	$29/2^-$	0.66(4)
1162.9	2.4(4)	3649.3	$(27/2^+)$	→	$25/2^-$	

The 1136- and 1730-keV γ rays feed the $33/2^-$ level at 2769 keV whereas the 1241-keV transition connects the 4910-keV state in Band 3 to the 3670-keV $37/2^-$ one in Band 2. Due to the weak population of the above proposed levels, spin-parity assignments were not feasible.

B. ^{199}Hg

Previous work on ^{199}Hg [5,20] had established positive-parity states up to spin $25/2\,\hbar$, negative-parity levels up to $31/2\,\hbar$, and excitation energies 2106 and 3067 keV, respectively. The decoupled positive-parity sequence labeled Band 2 in Fig. 2 is newly established up to an excitation energy of 8.5 MeV. The negative-parity semidecoupled Bands 3 and 4 are extended up to a probable spin $39/2\,\hbar$. Detailed results are described below.

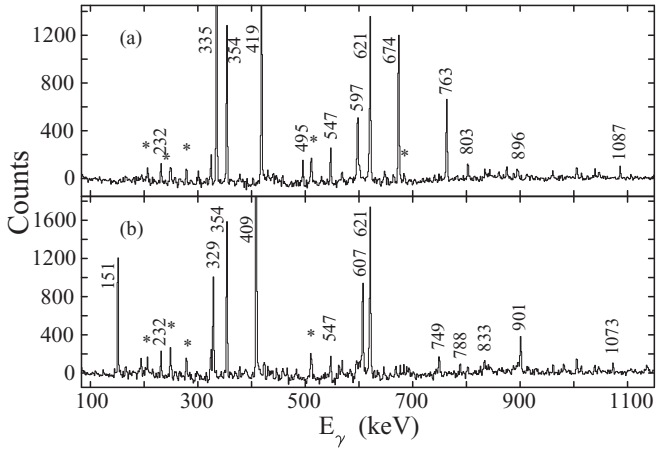

FIG. 3. Representative spectra showing transitions in ^{197}Hg in a sum of double-coincidence gates. In (a), the gates are on the 354–763-, 354–674-, 621–763-, and 621–674-keV γ transitions. In (b), the gates are on the 354–329-, 354–607-, 621–329-, and 621–607-keV γ transitions. The peaks marked with asterisks indicate contaminant γ rays or ones which could not be placed in the level scheme.

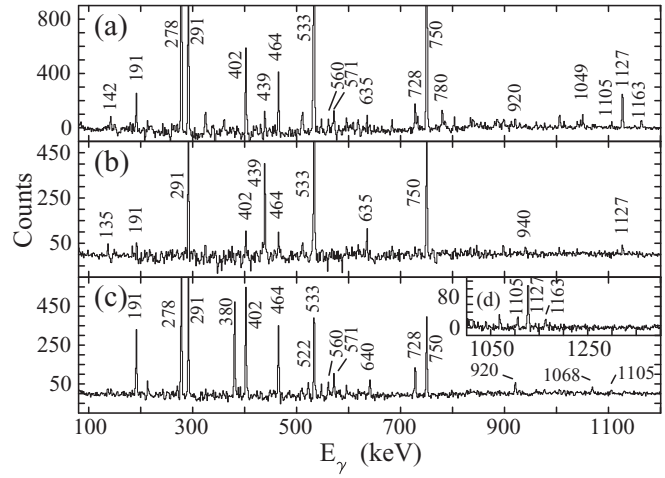

FIG. 4. Representative spectra showing transitions in ^{199}Hg: (a) Sum of double-coincidence gates with one gate on the 291-, 533-, and 750-keV γ rays and the other on the 380-keV transition, (b) sum of double-coincidence gates with one gate on the 291-, 533-, and 750-keV γ rays and the other on the 522-keV transition, (c) sum of double-coincidence gates with one gate on the 291-, 533-, 750-, and 380-keV γ rays and the other on the 1127-keV transition, and (d) double-coincidence gate on the 291- and 402-keV γ rays.

1. Positive-parity Bands 1 and 2

Previous work on ^{199}Hg [5,20] had led to the identification of positive-parity levels up to spin $25/2\,\hbar$ and excitation energy 2106 keV, labeled Band I in Fig. 2. This sequence is confirmed in the present work. The decoupled positive-parity sequence labeled Band 2 in Fig. 2 is newly identified up to an excitation energy around 8.5 MeV. There is no direct decay branch observed between Bands 1 and 2. Possible reasons for the absence of linking transitions will be discussed later. Band 2 is observed to deexcite to the negative-parity Bands 3 and 4 via several high-energy transitions: 885, 977, 1015, 1127, and 1163 keV, all of which are assigned $E1$ multipolarity (Fig. 2). The observation of the 1163-keV γ ray in the double-coincidence gate on the 291- and 402-keV transitions and its absence in the ones involving the 1127-keV γ ray as one of the gates (Fig. 4) imply a parallel placement of the 1127- and 1163-keV transitions. The 1127-keV γ ray, which feeds the $29/2^-$ level in Band 3, is determined to have dipole nature from the DCO analysis (Table II) leading to a probable spin assignment of $31/2\,\hbar$ for the 3891-keV level. The positive-parity assignment for this and other levels in Band 2 is based on the systematic behavior observed in even-Hg isotopes up to ^{200}Hg [28] and will be addressed in the next section. The 191-keV γ ray is observed to be in coincidence with the 1127-keV transition and is also deduced to have dipole nature based on its DCO ratio (Table II). The 150-, 885-, 977-, 1015-, and 1163-keV transitions are quite weak, however, their placement in the level scheme is unambiguously validated by observed coincidence relationships, some of which are described below. For example, these transitions and the ones in Band 2 are absent in the double-gated coincidence spectrum on the 532- and 533-keV γ rays. Furthermore, the 1163-keV transition is observed to be in coincidence with only the γ rays below the $25/2^-$ level, whereas the 1127-keV one is seen to be in coincidence with those below the $29/2^-$ state. The 191-keV transition is observed to be in coincidence with the 1127-keV γ ray, whereas the 150-keV one is in coincidence with the 191-keV but not the 1127-keV γ ray. The observed coincidence relationships also lead to the inference of an unobserved 92-keV transition between the 3741- and 3649-keV levels. The nonobservation of this transition may be understood in terms of its low intensity and expected large conversion coefficient. The 402- and 464-keV γ rays, which are placed in cascade above the $33/2^+$ level, are determined to have quadrupole character from DCO ratios and are, therefore, assigned $E2$ multipolarity. The 728-, 640-, 571-, 560-, and 1105-keV transitions are in coincidence with each other and the 402- and 464-keV γ rays and are placed using intensity considerations. Although unambiguous spin assignments for the levels deexcited by these transitions were not possible, $E2$ multipolarity is assumed leading to a spin-parity $I^\pi = (61/2^+)$ for the highest level established in this sequence. The 960- and 920-keV γ rays are identified to feed the $37/2^+$ and $41/2^+$ states in Band 2, respectively. The 448-keV transition feeds the 5868-keV level deexcited by the 920-keV γ ray. The 448- and 920-keV transitions are assumed to have $E2$ multipolarity, similar to other γ rays in cascade in Band 2.

2. Negative-parity Bands 3 and 4

Negative-parity levels up to spin $31/2\,\hbar$ and excitation energy 3067 keV had been previously identified [20]. In the present work, the negative-parity semidecoupled Bands 3 and 4 are extended up to spin $39/2\,\hbar$ and excitation energy 4642 keV. The 532- and 780-keV transitions are newly established in Band 3, whereas the 635- and 940-keV γ rays are assigned to Band 4; $E2$ multipolarity is assumed for these γ rays in view of the regular band structure. Clear evidence for

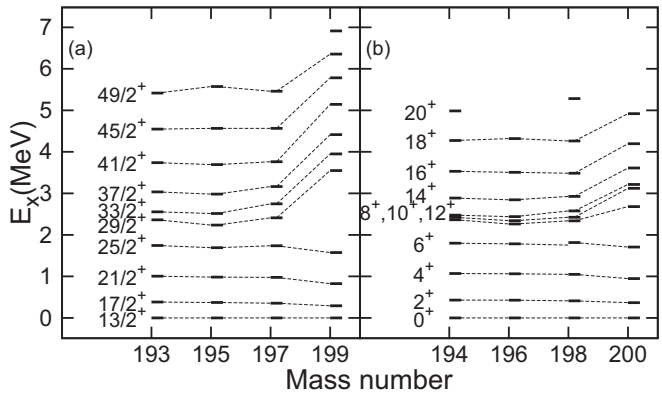

FIG. 5. Systematics of levels in (a) the positive-parity yrast band in ^{193,195,197,199}Hg and (b) the ground-state positive-parity band in ^{194,196,198,200}Hg. It may be noted that the excitation energy of the $13/2^+$ state in the odd-A isotopes is offset by an amount equal to its excitation energy (typically several hundred keV) to facilitate the comparison.

the presence of the 532-keV γ ray, which otherwise cannot be resolved from the $21/2^+ \rightarrow 17/2^+$ 533-keV transition, is obtained in double-gated spectra with gates on the 533-keV and other γ rays. The 135- and 142-keV transitions connect states in Bands 3 and 4. The presence of a $\Delta I = 1$, 61-keV transition connecting the $25/2^-$ and $23/2^-$ levels is inferred from observed coincidence relationships between the 278- and the 1068-keV γ rays.

IV. DISCUSSION

A. Decoupled positive-parity bands

Isotopes of Hg with $A = 190$–200 are characterized by oblate deformation near their respective ground states. A low-lying $I^\pi = 13/2^+$ spin isomer, arising from the occupation of the $i_{13/2}$ orbital by the unpaired neutron, is present in odd-A isotopes. With an increase in neutron number from $N = 110$ for ^{190}Hg to $N = 120$ for ^{200}Hg, the unpaired neutron occupies successively lower-Ω orbitals in the $i_{13/2}$ subshell up to $\Omega = 1/2$ in the case of ^{199}Hg. This leads to decoupled positive-parity rotational bands built on the one-quasineutron $13/2^+$ state in ^{197,199}Hg with the signature partner sequence being unfavored in energy. The similarity between the bands built on the $13/2^+$ level in odd-A Hg isotopes and those built on the ground state in even-A ones is quite striking as can be seen from the comparison provided in Fig. 5. It is evident that the energy systematics of the $I^\pi = 2^+$, 4^+, 6^+, and 8^+ levels in even-mass isotopes from $A = 194$–200 track quite closely with that of the $I^\pi = 13/2^+$, $17/2^+$, $21/2^+$, and $25/2^+$ states in the one-quasineutron decoupled sequences in the odd-mass isotopes from $A = 193$–199.

The similarity in the level structure of even- and odd-A isotopes observed at low spin becomes less evident at higher spin. In even-A isotopes, the $I^\pi = 8^+$, 10^+, and 12^+ levels are quite closely spaced. In contrast, the analogous $I^\pi = 29/2^+$, $33/2^+$, and $37/2^+$ levels have a higher-energy separation. It may also be noted that the discontinuity starts above $I^\pi = 6^+$ and $25/2^+$ levels in the even- and odd-A isotopes, respectively, creating a large energy gap to the next higher level, the magnitude of which is greater in the latter instance. These observations are explained later in the context of cranking calculations. Furthermore, a discontinuous increase in energy is observed beyond the $29/2^+$ and the 8^+ levels in ^{199}Hg and ^{200}Hg, respectively. In ^{200}Hg, this increase is attributed to the $i_{13/2}$ subshell being filled at $N = 120$ and a large gap in the single-particle energy levels beyond this neutron number which leads to the excitation of an $i_{13/2}$ neutron pair being more energetically expensive [28]. A similar explanation appears to be valid in the case of ^{199}Hg where the unpaired neutron occupies the $\Omega = 1/2$ orbital of the $i_{13/2}$ subshell and the energy of the $29/2^+$ and $33/2^+$ levels is elevated similar to that of the 8^+ and 10^+ states in ^{200}Hg.

Cranking calculations were performed using the ULTIMATE CRANKER code with standard Nilsson parameters [38] in order to understand shape evolution with spin and the aligned angular momentum as a function of rotational frequency deduced from the established level structure. The total energy surface plots indicate a near-oblate-deformed shape at $I^\pi = 21/2^+$ with a transition to a triaxial shape with reduced collectivity at $I^\pi = 33/2^+$ in ^{199}Hg (Fig. 6). The calculations suggest similar behavior in ^{197}Hg as well.

The rotation alignment of valence high-j nucleons is expected to generate high angular momentum in deformed nuclei. In this case, since the $i_{13/2}$ neutrons occupy low-Ω orbitals, the quasiparticle energy levels are expected to be strongly down-sloping with an increase in rotational frequency. The aligned angular momentum as a function of rotational frequency for odd- and even-mass isotopes is plotted in Fig. 7. It is evident that the first band crossing in even-A isotopes occurs at $\hbar\omega \approx 0.18$ MeV whereas that in odd-A ones occurs at $\hbar\omega \approx 0.22$ MeV (Fig. 7). The backbend is more pronounced in the even-mass isotopes as compared to the odd-mass ones. These observations can be explained through an inspection of the calculated neutron quasiparticle levels in ^{199}Hg (Fig. 8). The AB $i_{13/2}$ neutron crossing is evident around $\hbar\omega = 0.16$ MeV (Fig. 8) and is the one observed in even-A isotopes. This crossing is blocked on account of the Pauli principle in odd-A isotopes, however, the BC crossing is predicted at 0.26 MeV (Fig. 8). These predictions correlate reasonably well with the observed crossing frequencies in even- and odd-mass isotopes mentioned above. The interaction at the band crossing is expected to be stronger in the case of the BC crossing when compared to the AB one, in agreement with the less pronounced backbend observed in the experimental data for odd-A isotopes. This leads to increased energy spacing between the levels in the vicinity of the band crossing in the odd-A isotopes compared to the even-A ones. The band structures in ^{197,199}Hg built on the $33/2^+$ state are, therefore, assigned a $(\nu i_{13/2})^3$ decoupled configuration.

B. Semidecoupled negative-parity bands

The observation of semidecoupled bands in both even- and odd-mass isotopes of Pt and Hg is a common feature in this mass region. In even-A isotopes, these bands are built on a 2-qp configuration which has predominant neutron character

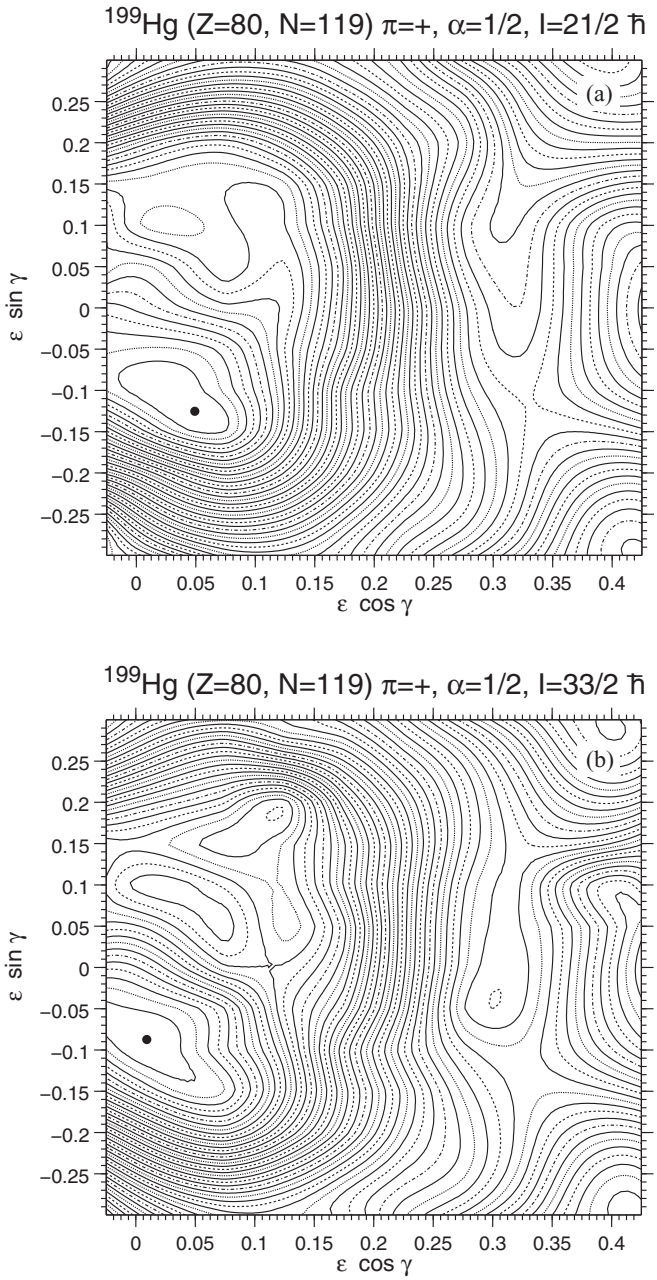

FIG. 6. Total energy surface plots for ^{199}Hg at $I^\pi = 21/2^+$ and $33/2^+$ calculated using the ULTIMATE CRANKER code [38]. The energy minima are located at $(\epsilon_2, \gamma) = (0.135, -69^\circ)$ for (a) $I^\pi = 21/2^+$ and at $(\epsilon_2, \gamma) = (0.088, -84^\circ)$ for (b) $I^\pi = 33/2^+$ in ^{199}Hg. Adjacent energy contours are spaced by 200 keV.

in Hg isotopes. The two quasineutrons involved are high-j $i_{13/2}$ and low-j neutrons either from the $p_{1/2}$, $p_{3/2}$, or $f_{5/2}$ orbitals. The coupling of the high- and low-j neutrons leads to a semidecoupled configuration and states with $I^\pi = 5^-$ and 7^- in even-A isotopes. In the odd-A ones where the unpaired neutron occupies the $i_{13/2}$ orbital, the semidecoupled band has a 3-qp configuration with one low-j and two $i_{13/2}$ neutrons. The levels analogous to the $I^\pi = 5^-$ and 7^- ones in even-A isotopes are those with $I^\pi = 21/2^-$ and $25/2^-$ in odd-A ones

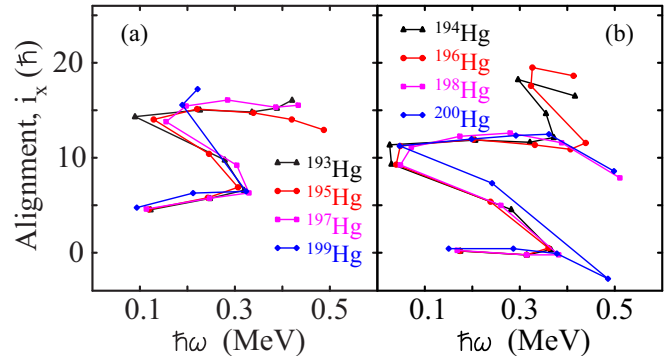

FIG. 7. Aligned angular momentum for the positive-parity bands in (a) ^{193,195,197,199}Hg and (b) ^{194,196,198,200}Hg. Inertial parameters $J_0 = 5\ \hbar^2\ \text{MeV}^{-1}$ and $J_1 = 68\ \hbar^4\ \text{MeV}^{-3}$ were obtained from a fit of low-spin members of the ground-state bands in even Hg isotopes with the Harris formula [39]. The first backbend in even- and odd-A isotopes is evident at $\hbar\omega \approx 0.18$ and 0.22 MeV, respectively.

since the second $i_{13/2}$ neutron can contribute only $\Omega = 11/2$ due to the Pauli principle.

A relatively regular structure is evident in the 3-qp semidecoupled bands in comparison to the 3-qp decoupled ones which may be attributed to the involvement of the low-j neutron in the former configuration. The observation of the unfavored signature of the semidecoupled sequence in ^{199}Hg is evident in the corresponding core ^{200}Hg [28] whereas its absence in ^{197}Hg is also reflected in ^{198}Hg [19]. The structure of Pt isotones is described in an accompanying paper [40].

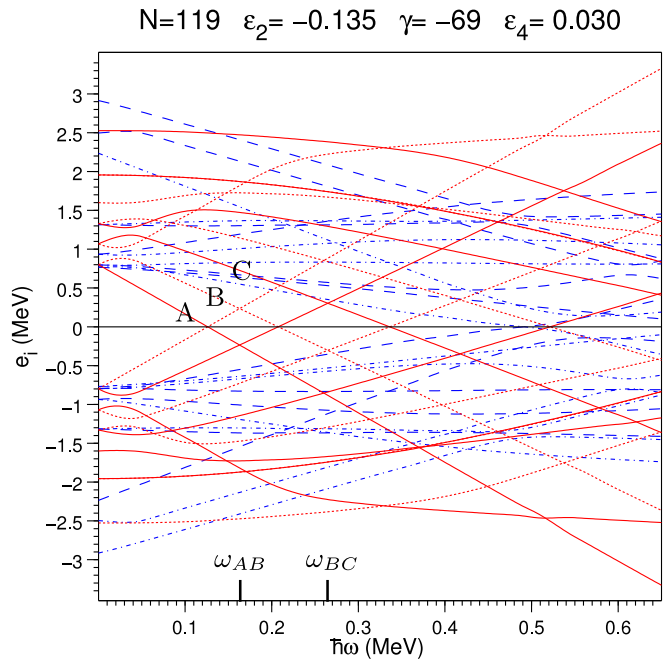

FIG. 8. Neutron quasiparticle energy levels in ^{199}Hg as a function of rotational frequency calculated using the ULTIMATE CRANKER code [38]. The predicted band crossings and respective frequencies are: 0.16 MeV (AB) and 0.26 MeV (BC). In ^{199}Hg, the AB crossing is blocked, therefore, the BC crossing is expected to be observed.

V. SUMMARY

Excited states in odd-A isotopes ^{197}Hg and ^{199}Hg up to high spin have been populated using multinucleon transfer reactions with a ^{209}Bi beam. Decoupled positive-parity sequences built on the $(\nu i_{13/2})^1$ and $(\nu i_{13/2})^3$ configurations are established. The 3-qp sequence in ^{199}Hg is newly identified whereas the one in ^{197}Hg is extended to higher spin. Several new transitions have been placed in the semidecoupled negative-parity sequences in both isotopes. At low spin, the evolution of structure in odd-mass isotopes is similar to the corresponding even-mass ones, however, at high spin, significant differences are noted arising from the different natures of band crossings and the associated interaction strengths. The experimental data are described well by ULTIMATE CRANKER calculations with standard Nilsson parameters and a change in shape from collective oblate to a triaxial one with reduced collectivity at high spin is indicated.

ACKNOWLEDGMENTS

We would like to thank I. Ahmad, J. P. Greene, A. J. Knox, D. Peterson, U. Shirwadkar, X. Wang, and C. M. Wilson for assistance during the experiment. S.K.T. would like to acknowledge support from the University Grants Commission, India under the Faculty Recharge Programme. This work was supported by the U.S. Department of Energy, Office of Science, Office of Nuclear Physics under Grants No. DE-FG02-94ER40848, No. DE-FG02-94ER40834, No. DE-FG02-97ER41033, and No. DE-FG02-97ER41041 and Contract No. DE-AC02-06CH11357. The research described here utilized resources of the ATLAS facility at ANL, which is a DOE Office of Science user facility.

[1] E. Ngijoi-Yogo *et al.*, Phys. Rev. C **75**, 034305 (2007).
[2] U. S. Tandel *et al.*, Phys. Rev. Lett. **101**, 182503 (2008).
[3] T. L. Khoo, F. M. Bernthal, C. L. Dors, M. Piiparinen, S. Saha, P. J. Daly, and J. Meyer-Ter-Vehn, Phys. Lett. **60**, 341 (1976).
[4] S. K. Saha, M. Piiparinen, J. C. Cunnane, and P. J. Daly, Phys. Rev. C **15**, 94 (1977).
[5] D. Proetel, D. Benson, Jr., A. Gizon, J. Gizon, M. R. Maier, R. M. Diamond, and F. S. Stephens, Nucl. Phys. A **226**, 237 (1974).
[6] D. Proetel, R. M. Diamond, and F. S. Stephens, Nucl. Phys. A **231**, 301 (1974).
[7] H. Beuscher, W. F. Davidson, R. M. Lieder, A. Neskakis, and C. Mayer-Böricke, Phys. Rev. Lett. **32**, 843 (1974).
[8] R. V. F. Janssens *et al.*, Phys. Lett. **131**, 35 (1983).
[9] I. G. Bearden *et al.*, Nucl. Phys. A **576**, 441 (1994).
[10] R. M. Lieder *et al.*, Nucl. Phys. A **248**, 317 (1975).
[11] K. Neergård, P. Vogel, and M. Radomski, Nucl. Phys. A **238**, 199 (1975).
[12] H. T. K. Neergård, P. Vogel, and A. Faessler, Nucl. Phys. A **279**, 1 (1977).
[13] P. J. Daly, J. C. Cunnane, S. W. Yates, and R. Hochel, in *Proceedings of the International Conference on Nuclear Physics, Munich, Germany, 1973*, edited by J. de Boer and H. J. Mang (North-Holland, Amsterdam, 1973), p. 193.
[14] R. F. Petry, R. A. Naumann, and J. S. Evans, Phys. Rev. **174**, 1441 (1968).
[15] J. C. Cunnane, R. Hochel, S. W. Yates, and P. J. Daly, Nucl. Phys. A **196**, 593 (1972).
[16] S. A. Hjorth, A. Johnson, T. Lindblad, L. Funke, P. Kemnitz, and G. Winter, Nucl. Phys. A **262**, 328 (1976).
[17] S. W. Yates, E. M. Baum, E. A. Henry, L. G. Mann, N. Roy, A. Aprahamian, R. A. Meyer, and R. Estep, Phys. Rev. C **37**, 1889 (1988).
[18] S. W. Yates, J. C. Cunnane, R. Hochel, and P. J. Daly, Nucl. Phys. A **222**, 301 (1974).
[19] C. Günther, H. Hübel, A. Kleinrahm, D. Mertin, B. Richter, W. D. Schneider, and R. Tischler, Phys. Rev. C **15**, 1298 (1977).
[20] D. Mertin, R. Tischler, A. Kleinrahm, R. Kroth, H. Hübel, and C. Günther, Nucl. Phys. A **301**, 365 (1978).
[21] S. A. Hjorth, I. Y. Lee, J. R. Beene, C. Roulet, D. R. Haenni, N. R. Johnson, F. E. Obenshain, and G. R. Young, Phys. Rev. Lett. **45**, 878 (1980).
[22] R. Kroth, K. Hardt, M. Guttormsen, G. Mikus, J. Recht, W. Vilter, H. Hübel, and C. Günther, Phys. Lett. **99**, 209 (1981).
[23] M. Guttormsen, Y. K. Agarwal, C. Günther, K. Hardt, H. Hübel, A. Kalbus, R. Kroth, G. Mikus, J. Recht, and P. Schüler, Nucl. Phys. A **383**, 541 (1982).
[24] M. Guttormsen, Y. K. Agarwal, K. P. Blume, H. Hübel, J. Recht, and P. Schüler, Nucl. Phys. A **398**, 119 (1983).
[25] H. Helppi, S. K. Saha, P. J. Daly, S. R. Faber, and T. L. Khoo, Phys. Rev. C **28**, 1382 (1983).
[26] H. Hübel, A. P. Byrne, S. Ogaza, A. E. Stuchbery, and G. D. Dracoulis, Nucl. Phys. A **453**, 316 (1986).
[27] D. Mehta, Y. K. Agarwal, K. P. Blume, S. Heppner, H. Hübel, M. Murzel, K. Theine, W. Gast, G. Hebbinghaus, R. M. Lieder, and W. Urban, Z. Phys. A **339**, 317 (1991).
[28] A. Görgen *et al.*, Eur. Phys. J. A **6**, 141 (1999).
[29] G. A. Jones *et al.*, Acta Phys. Pol. B **36**, 1323 (2005).
[30] Y. D. Fang *et al.*, Phys. Rev. C **84**, 017301 (2011).
[31] S. G. Wahid *et al.*, Phys. Rev. C **92**, 054323 (2015).
[32] S. K. Tandel *et al.*, Phys. Lett. B **750**, 225 (2015).
[33] R. Broda, M. A. Quader, P. J. Daly, R. V. F. Janssens, T. L. Khoo, W. C. Ma, and M. W. Drigert, Phys. Lett. B **251**, 245 (1990).
[34] W. Królas, R. Broda, B. Fornal, T. Pawłat, H. Grawe, K. H. Maier, M. Schramm, and R. Schubart, Nucl. Phys. A **832**, 170 (2010).
[35] I.-Y. Lee, Nucl. Phys. A **520**, c641 (1990).
[36] D. C. Radford, Nucl. Instrum. Methods Phys. Res., Sect. A **361**, 297 (1995).
[37] A. Krämer-Flecken, T. Morek, R. M. Lieder, W. Gast, G. Hebbinghaus, H. M. Jäger, and W. Urban, Nucl. Instrum. Methods Phys. Res., Sect. A **275**, 333 (1989).
[38] T. Bengtsson, Nucl. Phys. A **512**, 124 (1990).
[39] S. M. Harris, Phys. Rev. **138**, B509 (1965).
[40] S. G. Wahid *et al.*, Phys. Rev. C **100**, 014328 (2019).